

Dynamics of plasma gratings in atomic and molecular gases

M. Durand,^{1,2,*} A. Jarnac,¹ Y. Liu,¹ B. Prade,¹ A. Houard,¹ V. Tikhonchuk,³ and A. Mysyrowicz^{1,†}

¹Laboratoire d'Optique Appliquée, ENSTA ParisTech, Ecole Polytechnique, CNRS, 91761, Palaiseau, France

²Département d'Optique Théorique et Appliquée, ONERA, 91123, Palaiseau, France

³University of Bordeaux, CNRS, CEA, CELIA (Centre Lasers Intenses et Applications) UMR 5107, 33405, Talence, France

(Received 28 February 2012; published 13 September 2012)

The decay of the plasma grating formed at the intersection of two femtosecond filaments is measured in several molecular and atomic gases. The grating evolution is ruled by ambipolar diffusion in atomic gases and by a combination of ambipolar diffusion and collision-assisted free electron recombination in molecular gases. Electron diffusion and recombination coefficients are extracted for Ne, Ar, Kr, Xe, N₂, O₂, CO₂, and air at 1 bar.

DOI: [10.1103/PhysRevE.86.036405](https://doi.org/10.1103/PhysRevE.86.036405)

PACS number(s): 52.50.Jm, 42.65.Jx, 52.70.Kz

I. INTRODUCTION

Intense femtosecond laser pulses propagating in a neutral gas undergo a beam collapse if the incident pulse peak power exceeds a critical value, $P_{\text{cr}} \approx 0.15\lambda^2/n_0n_2$, where n_0 is the linear refractive index, n_2 the nonlinear index coefficient, and λ the wavelength of the laser pulse in vacuum [1,2]. The collapse is arrested by the defocusing effect due to multiphoton ionization of the gas. The ensuing dynamic competition between beam self-focusing and plasma defocusing gives rise to filamentation, a propagation regime characterized by a contracted pulse keeping a high intensity over long distances, leaving a thin weakly ionized plasma column in its wake [3]. Recently, much attention has been given to the interaction between two crossing filaments [4–8]. Because of field interference, a two-dimensional plasma grating is formed in the intersection region when two noncollinear filamentary pulses overlap in time. This grating plays an important role in the interaction between laser beams. For instance, the moving plasma grating formed by two intersecting filaments of slightly different central frequency is responsible for an important exchange of energy between the filaments [5]. A stationary grating formed with pulses of the same frequency can interrupt the progression of a filament [9] or it can redirect a third beam of different frequency [7,10]. Since the plasma grating persists well after the passage of the pulses, it provides a way to manipulate additional probe beams or filaments in a radiation free environment. The grating is periodic but anharmonic as the electron density created by the ionization process is a nonlinear function of the laser intensity. It is therefore important to measure its lifetime and understand the origin of its decay.

Recently, Shi *et al.* [11] have reported an exponential decay of the plasma grating formed in air by two UV filaments, with a lifetime on the order of 100 ps in air. However, as shown in this letter, the decay process cannot be expressed in most cases with a simple exponential law. In particular, the grating decay time may vary considerably in a given gas, depending on the grating fringe separation. Two distinct processes contribute to the grating decay: ambipolar diffusion and electron recombination. They have quite different characteristic times

and the laser beam crossing experiment allows assessing these processes in a parameter domain that has never been explored so far.

We have measured the plasma grating decay in several atomic and molecular gases at normal pressure. In atomic gases, we observe a decay that is dominated by diffusion. In molecular gases, both plasma recombination and diffusion contribute to the grating decay on a comparable time scale. From the measurements, we extract the coefficients of ambipolar diffusion and free electron recombination in Ne, Kr, Ar, Xe, N₂, O₂, CO₂, and air at atmospheric pressure.

II. EXPERIMENTAL SET-UP

The principle of the experiments is as follows (Fig. 1): In a first configuration A, two laser pulses at the same frequency ω enter a cell containing the gas at atmospheric pressure where they form two filaments that propagate in the y - z plane and intersect in the middle of the cell. A plasma grating is formed in the intersection region, as evidenced by the image of the plasma luminescence shown for air in Fig. 1(a). The main period of the observed fringe separation obeys well the relation $\Lambda = \lambda/[2 \sin(\phi/2)]$, where ϕ is the crossing angle. A weaker third probe beam at frequency 2ω , collinear with one of the filament forming pulses, is diffracted by the grating in the direction of the other filament. In order to satisfy the Bragg condition, the probe beam is diffracted by the second order anharmonic term of the grating profile $\Lambda_2 = \Lambda/2$. The diffracted signal is measured as a function of the delay between the grating forming pulses and the probe for three different crossing angles, $\phi = 7^\circ, 14^\circ$, and 90° . Both filamentary pulses ($\lambda = 800$ nm, duration 35 fs, pulse energy 1 mJ) are derived from the same chirped pulse amplification (CPA) Ti:Sa laser and are linearly polarized along x . The probe pulse (wavelength 400 nm, duration 35 fs, pulse energy 30 μ J), of the same polarization, is obtained by frequency doubling in a Beta Barium Borate crystal (BBO) of a fraction of the CPA laser output.

In a complementary experiment (configuration B), a collimated probe pulse at frequency ω propagates perpendicularly to the bidimensional fringe pattern formed by the two filaments crossing under angle $\phi = 7^\circ$ [see Fig. 1(b)]. In this in-line holographic imaging technique [12–14], the diffraction pattern due to the plasma bubble is recorded at a distance of 38 cm from the grating by a CCD camera as a function of the probe pulse

*Current address: Townes Laser Institute, CREOL, Orlando, FL 32816, USA.

†andre.mysyrowicz@ensta.fr

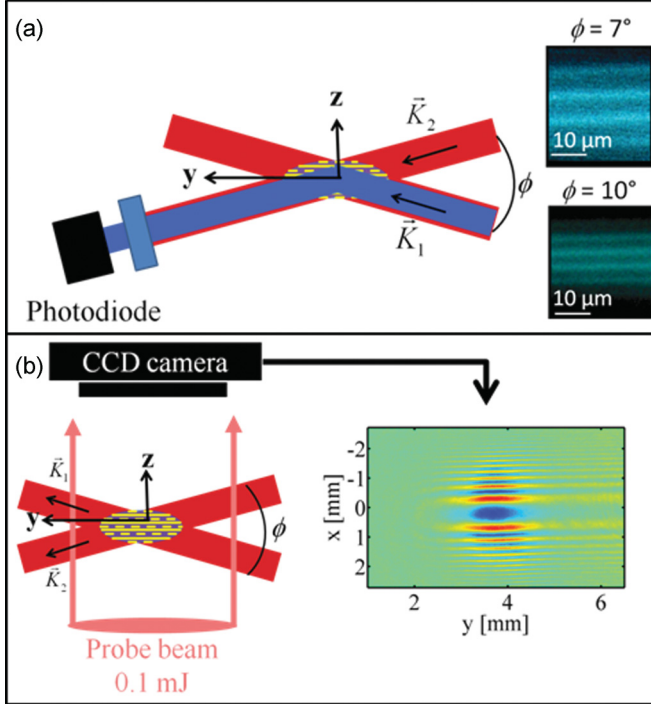


FIG. 1. (Color online) (a) Pump-probe set up (configuration A) used to study the decay of the plasma grating. The probe pulse at 400 nm propagates collinearly with one filament and is diffracted along the other filament. The luminescence of the plasma in air is also shown for two incident angles showing the formation of a grating. (b) Top view of the holographic imaging setup used to study the time evolution of the plasma (configuration B). The far field diffraction pattern of a probe pulse at 800 nm crossing the plasma area in O_2 with a delay of 4.5 ps is also shown.

delay. Here, the probe beam records the average free electron density through the concomitant variation of the refractive index. As the direction of the probe beam is parallel to the grating wave vector, there is no probe diffraction from the grating but only from the overall plasma filament.

III. RESULTS AND DISCUSSIONS

Figure 2 shows the amplitude of the diffracted probe signal seen in configuration A as a function of time in the case of argon and O_2 for three angles ϕ [15,16]. The same experiment has also been performed in Ne, Kr, Xe, N_2 , CO_2 , and air. In all atomic gases, there is a strong dependence of the signal diffracted by the grating with angle ϕ , but no significant decay of the plasma during the same time interval. By contrast, in molecular gases, a rapid decay of the plasma is measured, as shown for O_2 in Fig. 3(b). The strong dependence of the signal with ϕ in Fig. 2(a) can be qualitatively explained by the fact that the grating fringe spacing decreases with increasing angle ϕ . Closer fringe spacing leads to a reduction of the time necessary for a diffusive washout of the fringe pattern.

The electron diffusion in a weakly ionized plasma is strongly dependent on the relation between the electron Debye length, λ_D , electron mean free path, λ_{en} , and the grating period, Λ . For the expected conditions in the plasma filament (the electron temperature is of the order, or less than, 1 eV and the

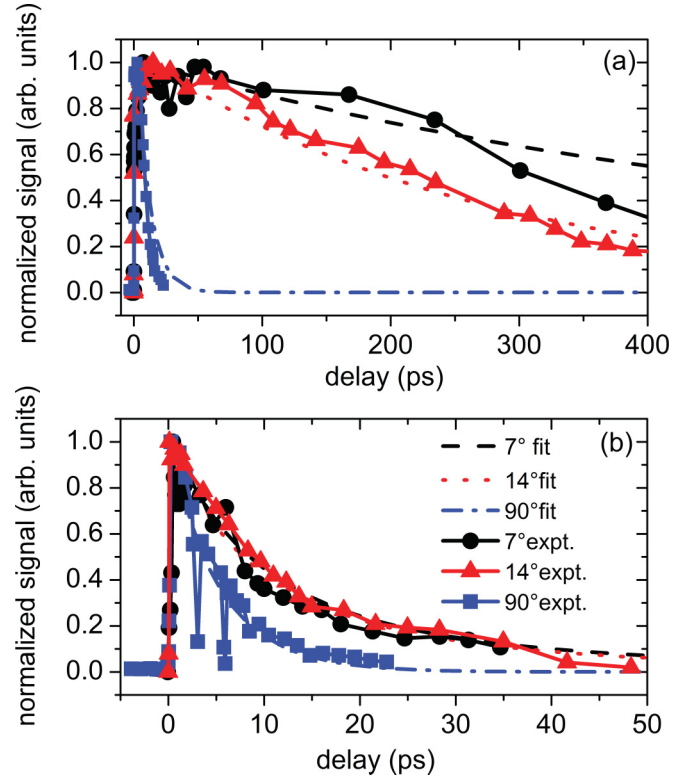


FIG. 2. (Color online) Normalized intensity of diffracted probe signal as a function of the delay τ (ps) in (a) argon and (b) O_2 for crossing angles ϕ of 7°, 14°, and 90°. Measurements performed in configuration A are represented by dots. Calculations are represented by continuous line.

electron density $\sim 10^{18} \text{ cm}^{-3}$) the electron Debye length, $\lambda_D \approx 0.07 \mu\text{m}$, and the electron mean free path, $\lambda_{en} \approx 0.15 \mu\text{m}$, are much smaller than the grating period Λ . Then a quasineutrality is maintained across the grating and the electron's diffusion is controlled by the ion mobility. As the ion temperature T_i is close to room temperature and is much smaller than the electron temperature, T_e , the ambipolar diffusion coefficient reads as $D_{am} \approx D_i(1 + T_e/T_i)$, where $D_i = kT_i\mu_i/e$ is the ion diffusion coefficient, k is the Boltzmann constant, μ_i is the ion mobility, and e is the elementary charge.

Plasma recombination can occur through collision-assisted electron-ion recombination and additionally through dissociative recombination in molecules. The dissociative recombination process corresponds to the collision of an electron with a molecular ion that results in two neutral atoms at the output, $e^- + M_2^+ \rightarrow M^* + M$. The corresponding cross section could be as high as 10^{-13} – 10^{-14} cm^2 at room temperature but it decreases by two to three orders of magnitude for $T_e \approx 1$ – 10 eV [17]. In the collision-assisted recombination process, the electron recombines on the parent ion with the assistance of a momentum conserving neutral atom or molecule: $e^- + M^+ + M \rightarrow M + M$. For an electron density n_e on the order of 10^{17} cm^{-3} (corresponding to the density in the peaks of interference fringes) and a neutral density $n_a = 2.7 \times 10^{19} \text{ cm}^{-3}$, the dissociative recombination time should be on the order of a few nanoseconds, while the collision-assisted recombination time should be in the subnanosecond range. Therefore the latter process dominates under our experimental

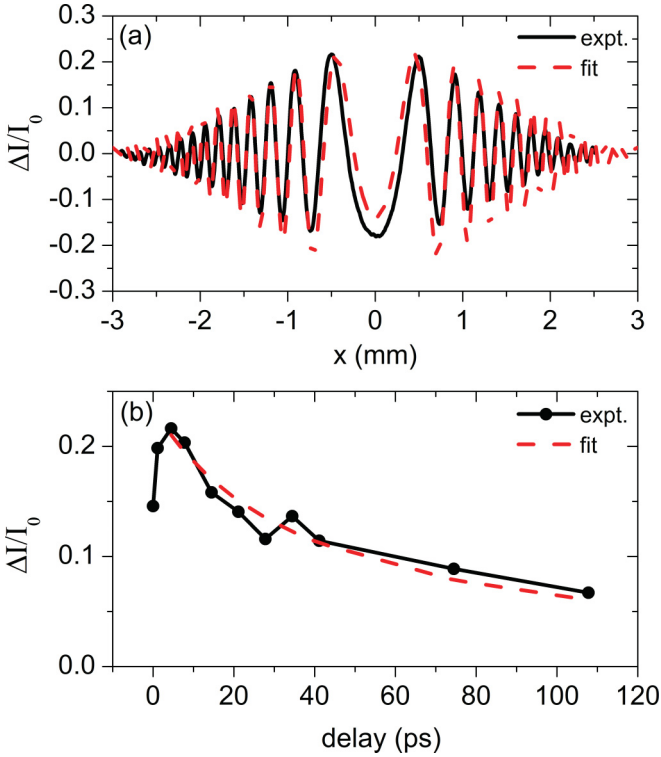


FIG. 3. (Color online) (a) Far field diffraction pattern of the probe beam in configuration B in O_2 ; fringes with maximum contrast are compared to calculations assuming a double Gaussian plasma profile. (b) Decay of the fringe contrast obtained in O_2 from successive diffraction patterns.

conditions. Indeed, several authors have already discussed the decay of plasma generated by laser filamentation in air in terms of predominant collision-assisted recombination [12,13].

The electron density evolution in the zone of the filament crossing can be described by the following equation:

$$\frac{\partial n_e}{\partial t} = n_a \sigma_M \{2I_0 [1 + \cos(qz)]\}^M + D_{\text{am}} \frac{\partial^2 n_e}{\partial z^2} - \beta n_e^2, \quad (1)$$

where $\beta = K n_a$ is the coefficient of electron recombination, $q = 2\pi/\Lambda$ is the main grating period, I_0 is the laser intensity in the filament, and σ_M is an effective cross section of strong field ionization. Here, we assume the plasma quasineutrality (the grating period is much larger than the electron mean free path and the electron Debye length) and weak ionization ($n_e \ll n_a$). The parameter M specifies the dependence of the ionization rate on the laser intensity. It is different from just a number of photons needed for ionization as it is supposed by the simple multiphoton ionization model. We use instead the power M extracted from the Perelomov, Popov, and Terent'ev (PPT) theory, which has been shown by Chin to correctly describe ionization of gases in the relevant intensity range [18,19]. We extract an effective number of simultaneously absorbed photons which varies from $M = 4$ for Kr to $M = 7$ for N_2 [18]. The plasma grating profile created by the multiphoton ionization is therefore highly anharmonic; it contains a series of harmonics N_q with $N \leq M$. The variation of the refraction index of the plasma, $\Delta N = -n_e/2n_{\text{cr}}$, is directly proportional to the ratio of the electron density to the plasma critical density,

$n_{\text{cr}} = \epsilon_0 m_e \omega_0^2 / e^2$, so that the grating evolution deduced from Eq. (1) contains M spatial harmonics.

As the laser pulse duration is much shorter than the grating relaxation time, we solve this equation in two steps. First we calculate the electron density distribution after the end of the laser pulse, while neglecting the two last terms in the right-hand side. The electron density reads $n_{e0}(z) = n_0 [1 + \cos(qz)]^M$, where $n_0 = 2^M n_a \sigma_M \int I_0^M dt$. In a second step, we solve the equation for n_e by considering only the last two terms of Eq. (1) with the function $n_{e0}(z)$ as the initial condition.

In atomic gases, the average electron density decays relatively slowly. In Ar, the grating amplitude corresponding to the main harmonic decreases by a factor of 2 in 1 ns while the second harmonic $q_2 = 2q$ requires less than 400 ps. This is a consequence of the fact that the rate of ambipolar diffusion rate increases as the square of the harmonic number. In molecular gases, the plasma recombination time is much shorter, comparable to the decay time of the grating measured in configuration A, so that both recombination and diffusion play a role in the relaxation of the plasma grating.

To find plasma parameters D_{am} , β , and the initial electron density n_0 , the measured grating decay curves for the three measured angles are best fitted for each gas. The initial conditions for solving Eq. (1) are obtained from fringe contrast measurements at different delays in configuration B, as discussed in details in Ref. [12]. Figure 3(a) shows an example of the far field image of the diffracted probe beam in O_2 measured at a probe delay of 4.5 ps. From a best fit of the fringe profile across coordinate x at maximum contrast at a given delay, the electron density at the corresponding time can be extracted. Then by changing the delay of the probe beam τ , the decay of the plasma is obtained, allowing extraction of the coefficient β and by extrapolation the initial density n_0 . Typically the initial electron density is on the order of 10^{17} – 10^{18} cm^{-3} . This value is in agreement with that calculated using the PPT theory [18,19], under the assumption of a complete interference between the two crossing laser fields. The numerical fitting procedure is stringent for molecular gases, since for a given set of parameters D_{am} and β , the diffraction patterns in configuration A and B as well as their time dependence must be reproduced. Extracted values of β and D_{am} are given in Table I for several atomic and molecular gases. There is good agreement between diffusion coefficients D_{am} from our experiments and ambipolar diffusion coefficients D_a extracted from mobility measurements. To calculate D_a we use $T_i = 300$ K, $T_e = 0.5$ eV, typical of filaments [20], and μ_i values are taken from the literature [21].

The constant K appearing in the recombination coefficient was determined at a very low pressure and at 300 K in He [22] (10^{-26} to 10^{-27} cm^6/s), O_2 [23] ($K \approx 10^{-30}$ cm^6/s), and Ne ($K \approx 10^{-27}$ cm^6/s) [24]. The present experiment gives for the first time a value of K for several gases at atmospheric pressure.

From Table I, one can see that atomic gases have a much lower recombination rate than molecular gases. We note, however, that Ne recombines faster than other atomic gases. We attribute this efficient dissociative recombination to rapid dimer formation. The extracted dissociation coefficient is consistent with the value reported in Ref. [24].

TABLE I. Plasma parameters determined from the dynamics of the plasma grating: The parameters D_{am} , n_0 , and β are obtained from best fitting the time dependence of the probe signal by the solutions of Eq. (1). The parameter K is calculated from the relation $\beta = Kn_a$, and the ambipolar diffusion coefficients are given for comparison by using the plasma parameters expected in the filament [20,21].

	Ne	Ar	Kr	Xe	O ₂	Air	CO ₂	N ₂
$D_a = D_i(1 + \frac{T_e}{T_i})$ (cm ² /s)	2.2	0.84	0.47	0.3	1.2	0.71	0.44	0.94
D_{am} (cm ² /s)	1	0.84	0.52	0.3	1.1	0.25	0.44	0.6
n_0 (cm ⁻³)	7.4×10^{17}	3.3×10^{18}	1.8×10^{18}	8.7×10^{17}	1.2×10^{18}	1.3×10^{18}	9×10^{17}	1.3×10^{18}
β (cm ³ /s)	6.4×10^{-9}	1.8×10^{-10}	9.5×10^{-10}	1.7×10^{-9}	4.1×10^{-8}	5.3×10^{-8}	1.8×10^{-7}	3.3×10^{-8}
K (cm ⁶ /s)	2.3×10^{-28}	6.6×10^{-30}	3.5×10^{-29}	6.3×10^{-29}	1.5×10^{-27}	2×10^{-27}	6.7×10^{-27}	1.2×10^{-27}

IV. CONCLUSIONS

To conclude, we have studied the dynamics of the plasma grating created by two intercepting filaments in different gases. The grating fringe evolution is dominated by ambipolar diffusion in atomic gases and by a combination of diffusion and recombination in molecular gases. The study of the plasma grating evolution provides a simple technique to determine

several characteristics of this unusual type of plasma which is dense but weakly ionized.

ACKNOWLEDGMENTS

We acknowledge fruitful discussions with Dr B. Forestier, technical help from J. Carbonnel, A. Dos Santos, and Dr. J. Gautier; we also acknowledge financial support from DGA.

-
- [1] V. I. Talanov, *Radiophysics* **9**, 138 (1965).
[2] P. L. Kelley, *Phys. Rev. Lett.* **15**, 1005 (1965).
[3] A. Couairon and A. Mysyrowicz, *Phys. Rep.* **441**, 47 (2007).
[4] A. C. Bernstein, M. McCormick, G. M. Dyer, J. C. Sanders, and T. Ditmire, *Phys. Rev. Lett.* **102**, 123902 (2009).
[5] Y. Liu, M. Durand, S. Chen, A. Houard, B. Prade, B. Forestier, and A. Mysyrowicz, *Phys. Rev. Lett.* **105**, 055003 (2010).
[6] X. Yang, J. Wu, Y. Peng, Y. Tong, P. Lu, L. Ding, Z. Xu, and H. Zeng, *Opt. Lett.* **34**, 3806 (2009).
[7] X. Yang, J. Wu, Y. Tong, L. Ding, Z. Xu, and H. Zeng, *Appl. Phys. Lett.* **97**, 071108 (2010).
[8] S. Suntsov, D. Abdollahpour, D. G. Papazoglou, and S. Tzortzakis, *Appl. Phys. Lett.* **94**, 251104 (2009).
[9] Y. Liu, M. Durand, A. Houard, B. Forestier, A. Couairon, and A. Mysyrowicz, *Opt. Commun.* **284**, 4706 (2011).
[10] M. Durand, Y. Liu, B. Forestier, A. Houard, and A. Mysyrowicz, *Appl. Phys. Lett.* **98**, 121110 (2011).
[11] L. Shi, W. Li, Y. Wang, X. Lu, L. Ding, and H. Zeng, *Phys. Rev. Lett.* **107**, 095004 (2011).
[12] G. Rodriguez, A. R. Valenzuela, B. Yellampalle, M. J. Schmitt, and K.-Y. Kim, *J. Opt. Soc. Am. B* **25**, 1988 (2008).
[13] S. Tzortzakis, B. Prade, M. Franco, and A. Mysyrowicz, *Opt. Commun.* **181**, 123 (2000).
[14] J. Wahlstrand, Y. Chen, Y. H Cheng, S. Varma, and H. Milchberg, *IEEE J. Quantum Electron.* **48**, 760 (2012).
[15] The sharp dips observed after 3 ps and 5.8 ps for $\phi = 90^\circ$ are due to spontaneous revivals of the refractive index [15] which diffract the probe pulse before it reaches the grating volume. For clarity, the dips observed at other angles ϕ have been removed.
[16] E. T. J. Nibbering, G. Grillon, M. A. Franco, B. S. Prade, and A. Mysyrowicz, *J. Opt. Soc. Am. B* **14**, 650 (1997).
[17] A. I. Florescu and J. B. A. Mitchell, *Phys. Rep.* **430**, 277 (2006).
[18] S. L. Chin, *Advances in Multiphoton Processes and Spectroscopy*, edited by S. H. Lin, A. A. Villaeys, and Y. Fujimura (World Scientific, Singapore, 2004), Vol. 16, p. 249.
[19] A. M. Perelomov, V. S. Popov, and M. V. Terent'ev, *Sov. Phys. JETP* **23**, 924 (1966).
[20] P. Sprangle, J. R. Peñano, B. Hafizi, and C. A. Kapetanakis, *Phys. Rev. E* **69**, 066415 (2004).
[21] E. U. Condon and H. Odishaw, *Handbook of Physics*, 2nd ed. (McGraw Hill, New York, 1967).
[22] J. Berlande, M. Cheret, R. Deloche, A. Gonfalone, and C. Manus, *Phys. Rev. A* **1**, 887 (1970).
[23] L. M. Chanin, A. V. Phelps, and M. A. Biondi, *Phys. Rev. Lett.* **2**, 344 (1959).
[24] R. N. Bhawe and R. Cooper, *Aust. J. Phys.* **48**, 503 (1995).